Ultrasound-enabled SIMO Channel for Targeted Brain Cancer Chemotherapy

Mohammad Zoofaghari*,†, Martin Damrath‡, Mladen Veletić†,‡, Ilangko Balasingham†,‡
*Department of Electrical Engineering, Yazd University, Yazd, Iran
†The Intervention Centre, Technology and Innovation Clinic, Oslo University Hospital, Oslo, Norway
‡Department of Electronic Systems, Norwegian University of Science and Technology, Trondheim, Norway

***Abstract*—Treating brain diseases with therapeutic particles imposes significant challenges as particles are usually too large to traverse the gaps between endothelial cells in the blood-brain barrier (BBB). Focused ultrasound (FUS) for disruption of the BBB has been proposed as a remedy. However, the extent of disruption and the efficiency of the particle delivery to the regions of interest are highly dependent on FUS sonication parameters. This study investigates the effects of not only FUS sonication parameters but also the therapeutic particle administration scheme by exploiting communication-theoretic channel modeling. Specifically, the particle pathways from blood vessels to hallmarked spots in the brain interstitial space are abstracted as a single-input-multiple-output (SIMO) channel. The channel outputs are then examined through the lenses of communication-theoretic measures such as channel gain, transmission efficiency, signal-to-noise ratio, and bit error ratio. The numerical results are displayed utilizing the available clinical data on six patients with brain cancer. The results show that the proposed approach could be exploited in future studies to maximize the efficacy of the treatment and minimize adverse effects.**

***Index Terms*—Focused ultrasound, drug delivery, SIMO molecular communication, blood-brain barrier.**

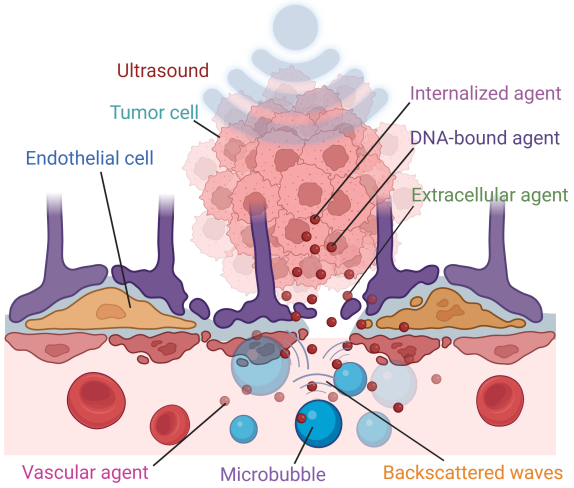

Fig. 1: Microbubble-based focused ultrasound mechanism for BBB disruption.

I. Introduction

Central nervous system diseases, such as Alzheimer's, tremors, and brain cancers like Glioblastoma, have significantly impacted humanity, often leading to life disruption or even termination. Drug delivery to the brain is primarily constrained by the Blood-Brain Barrier (BBB) [1]. The blood vessels that supply the central nervous system possess unique properties, collectively known as the blood-brain barrier, which tightly control the movement of ions, molecules, and cells between the blood and the brain. While molecules of a certain size can pass through the BBB, drug particles are usually too large to traverse the gaps between endothelial cells. In other words, conventional chemotherapeutic agents face significant obstacles when reaching brain tissues via BBB-based channels.

To overcome this challenge, an ultrasound-enabled channel has been proposed to disrupt the BBB transiently [2]. The extent of the disruption is highly dependent on various sonication parameters and the ultrasound signal path from the transducer on the skull to the targeted area. Additionally, to enhance the ultrasound effect, microbubbles can be administrated intravenously before sonication [3]. These ultrasound agents interact with the ultrasound waves and produce some microstreams toward the vessel walls due to the cavitation resulting in widened pores between endothelial cells, Fig. 1. The dosage and infusion schedule of microbubbles largely determine the intensity and timing of BBB disruption caused by the backscattered waves from these microbubbles.

A comprehensive review of research papers investigating the influence of acoustic parameters on the efficacy and safety of opening the BBB has been conducted by Gandhi et al. in their 2022 study [4]. This review includes the examination of various parameters, such as transducer frequency, peak negative pressure, burst duration, pulse repetition frequency, the number of sonications per session, and the number of treatment sessions, based on more than 100 preclinical and clinical studies. The paper also provides typical values for these parameters and discusses commercially available microbubble formulations. The effect of an acoustic parameter could be evaluated through the histological assessment of the treated tissue in the animal experiments. For example, Shin et al. [5] measured the extravasation of Evan blue (a dye commonly used in biological research to assess vascular permeability) in preclinical experiments under various parameter values, revealing that acoustic pressure and burst duration have the most significant impact on enhancing BBB permeability. For clinical trials, Dynamic Contrast-Enhanced Magnetic Resonance Imaging (DCE-MRI) is usually exploited to measure the macroscopic permeability enhancement of BBB due to ultrasound exposure. For example, the effect of three values of the mechanical index (peak acoustic pressure over

square root of center frequency) is investigated in [6] and the transvascular rate coefficients are reported for 6 patients under Focused UltraSound (FUS) treatment.

The microbubble and drug injection schemes are influential on the treatment efficacy as well as the acoustic parameters. Lapin et al. [7] compared the effects of bolus injection and microbubble infusion in BBB disruption, particularly in multi-target sonication scenarios. This study demonstrated that, with the same microbubble dosage, infusion experiments resulted in more consistent BBB opening in mice due to reduced systematic microbubble clearance at sequentially sonicated points. Additionally, [8] used mathematical modeling to investigate the localized delivery of doxorubicin to brain tumors. It explored the effects of multiple sonications in a treatment session and the duration of drug infusion, revealing an optimal doxorubicin infusion time that maximizes the transport of agents across the cell membrane.

In this paper, we investigate a molecular communication (MC) framework to appraise the effect of sonication parameters as well as the therapeutic agents administration scheme on the drug delivery to brain tumors. Over recent years, molecular communication has emerged as a crucial paradigm for intrabody communication. One of its most significant applications lies in targeted drug delivery [9], where aspects related to drug release (interpreted as the transmitter), the medium between release and targeted cells (the channel), and the receiving cells (the receiver) can be tailored using communication concepts. We interpret the pathway of the therapeutic agent from the capillary to the tumor cell DNAs through the BBB as channel in which the ultrasound exposure can shape the channel output. This allows us to utilize the communication theorem to adjust the channel parameters to align with the input signal (infused drug), maximizing the drug efficacy. Additionally, it can be employed to simulate an off-target channel to reduce unintended drug delivery to the periphery of the tumor.

Ultrasound equipment serves as an external controller of the proposed MC system. Externally controllable MC system has been investigated before considering various physics. For example, [10] established a bio-nanomachine to bio-nanomachine interface between intrabody and extrabody MC systems in which the timing and location of in-body processes are controlled. Also, stimulating of the proteins by the terahertz waves is introduced in [11] to integrate external electromagnetic signals with an intrabody MC system. Electromagnetic waves can trigger the proteins to activate a biochemical event in the target cells.

In the cases of brain cancer, targeting the multiple spots on the tumor might be necessary to achieve sufficient drug delivery to the whole of the tumor. Sonication of each part on the tumor enables a pathway of drug delivery to that part and the number of sonication spots determines the number of outputs in a single-input multiple-output (SIMO) channel. The time delay between the spots sonication substantially regulates the channel outputs that was not addressed in the previous studies. We explore how the response of the described channels can be modulated using FUS and elaborate on how this scenario corresponds to an externally controllable SIMO communication system.

The BBB opening could be assessed by the MRI contrast agents e.g. gadolinium-diethylenetriamine penta-acetic acid (Gd-DTPA). The permeability enhancement of BBB due to ultrasound exposure depends on the size of administrated particles. Therefore, we can not evaluate the FUS-mediated treatment based on transvascular rate measured for Gd-DTPA as the therapeutic agents size could be quite different. Here we exploit a scaling function to get the transvascular rate values fitted to the drug species. This adjustment allows us to predict the system's performance without the need to directly measure the drug response.

In the following, we describe a model for the proposed SIMO system and characterize the channel through newly defined measures inspired by classical communications. The numerical results are represented based on data provided by a clinical trial of FUS-based chemotherapy for brain cancer.

II. System Model

Fig. 2 illustrates the system model we consider for the predefined SIMO channel. In this representation, $h_n(t)$ characterizes the ultrasound-enabled channel for each spot, depicting how therapeutic agents traverse the BBB and are absorbed by the target cells when a bolus injection (approximating an impulse input) is administered. Therefore, the nature of $h_n(t)$ is substantially influenced by the permeability of brain capillaries, which, in turn, is primarily dictated by factors such as tumor type, location, and the vascular network present at each specific spot. The number of sonication spots directly corresponds to the number of system outputs, and the output of each channel can be manipulated by adjusting various ultrasound signal parameters, and evaluated knowing its unique properties. The input to this system is represented by the

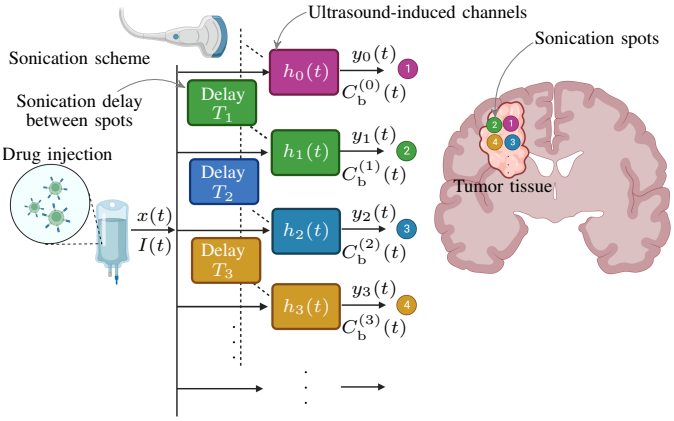

Fig. 2: Channel model of the proposed SIMO system. Here $C_b^{(n)}(t)$ stands for the concentration of DNA-bound agent for n^{th} channel.

drug infusion function $I(t)$, which is defined by the drug dosage and injection schedule. Additionally, we have included delay blocks in this schematic to illustrate the adjustable delay between two sequentially sonicated spots.

Extensive research has been conducted on the pharmacodynamics of the BBB and the recipient cells, focusing on both transvascular and extracellular transport [10], [12], [13], as well as the transmembrane and DNA binding dynamics [10], [13]. These studies have established models based on a set of ODEs that describe the drug's pathway from the bloodstream to the cell nucleus, primarily for a single-target pathway. However, in the current context of multi-target scenario, it is necessary to update the model to consider the cumulative impact of transvascular transport through different channels in the dynamics of vascular agents as follows:

$$\frac{\mathrm{d}C_{\mathrm{v}}(t)}{\mathrm{d}t} = \sum_{n=0}^{N-1} -K_{\mathrm{tv}}^{(n)}(t)(C_{\mathrm{v}}(t) - C_{\mathrm{e}}^{(n)}(t)) - K_{\mathrm{d}}^{\mathrm{v}} C_{\mathrm{v}}(t) + I(t), \tag{1}$$

$$\frac{\mathrm{d}C_{\mathrm{e}}^{(n)}(t)}{\mathrm{d}t} = K_{\mathrm{tv}}^{(n)}(t)(C_{\mathrm{v}}(t) - C_{\mathrm{e}}^{(n)}(t)) - \frac{VC_{\mathrm{e}}^{(n)}(t)d_{\mathrm{c}}}{C_{\mathrm{e}}^{(n)}(t) + K_{\mathrm{e}}\alpha} + \frac{VC_{\mathrm{i}}^{(n)}(t)d_{\mathrm{c}}}{C_{\mathrm{i}}^{(n)}(t) + K_{\mathrm{i}}(1-\alpha)} - K_{\mathrm{d}}^{\mathrm{e}} C_{\mathrm{e}}^{(n)}(t), \tag{2}$$

$$\frac{\mathrm{d}C_{\mathrm{i}}^{(n)}(t)}{\mathrm{d}t} = \frac{VC_{\mathrm{e}}^{(n)}(t)}{C_{\mathrm{e}}^{(n)}(t) + K_{\mathrm{e}}\alpha} - \frac{VC_{\mathrm{i}}^{(n)}(t)}{C_{\mathrm{i}}^{(n)}(t) + K_{\mathrm{i}}(1-\alpha)} - V_{\mathrm{b}} C_{\mathrm{i}}^{(n)}(t), \tag{3}$$

$$\frac{\mathrm{d}C_{\mathrm{b}}^{(n)}(t)}{\mathrm{d}t} = V_{\mathrm{b}} C_{\mathrm{i}}^{(n)}(t). \tag{4}$$

The key elements of the model include concentration variables, i.e. $C_{\mathrm{v}}(t)$, $C_{\mathrm{e}}^{(n)}(t)$, $C_{\mathrm{i}}^{(n)}(t)$, $C_{\mathrm{b}}^{(n)}(t)$, kinetics parameters, i.e. V, K_{e}, K_{i}, V_{b}, $K_{\mathrm{d}}^{\mathrm{v}}$, $K_{\mathrm{d}}^{\mathrm{e}}$, the biological factors, i.e. d_{c}, α, ultrasound-related parameter i.e. $K_{\mathrm{tv}}^{(n)}(t)$ and drug infusion function i.e. $I(t)$. $C_{\mathrm{v}}(t)$ represents vascular agent concentration, $C_{\mathrm{e}}^{(n)}(t)$ is for extracellular agents, $C_{\mathrm{i}}^{(n)}(t)$ pertains to internalized agents, and $C_{\mathrm{b}}^{(n)}(t)$ indicates the concentration of DNA-bound agents for n^{th} channel where N is the number of the channels (see Fig. 2). V is the rate of transmembrane transport and K_{e} and K_{i} serve as the Michaelis constant for transmembrane transport. Additionally, V_{b} signifies the binding rate of particles to DNA, particularly relevant for certain drugs like doxorubicin. $K_{\mathrm{d}}^{\mathrm{v}}$ accounts for drug excretion by the kidney, liver and etc, while $K_{\mathrm{d}}^{\mathrm{e}}$ represents extracellular degradation, indicating how quickly particles exit the area of interest. d_{c} denotes tumor cell density, and α signifies the volume fraction of extracellular matrix.

$K_{\mathrm{tv}}^{(n)}(t)$ can be adjusted by ultrasound exposure. It denotes the transvascular rate of the agent for n^{th} channel that is usually fitted to an exponential function given by

$$K_{\mathrm{tv}}^{(n)}(t) = \begin{cases} (K_{\mathrm{tv}}^{0,(n)} - K_{\mathrm{tv}}^{\mathrm{b}}) \times e^{-\frac{t-t_0-nT}{R}} + K_{\mathrm{tv}}^{\mathrm{b}} & \text{if } t > t_0 + nT, \\ K_{\mathrm{tv}}^{0,(n)} & \text{if } nT < t \le nT + t_0, \\ K_{\mathrm{tv}}^{\mathrm{b}} & \text{otherwise,} \end{cases} \tag{5}$$

where we considered the same time delay between sequential sonication of spots, $T_1 = T_2 = \cdots = T$, and $K_{\mathrm{tv}}^{\mathrm{b}}$ stands for the baseline value of the transvascular rate function. We assume that each spot is sonicated for t_0 minutes for which the transvascular rate increases from the baseline value to $K_{\mathrm{tv}}^{0,(n)}$ for n^{th} channel. After stopping sonication, $K_{\mathrm{tv}}^{(n)}(t)$ demonstrates the BBB closure with the time constant of R. $K_{\mathrm{tv}}^{(n)}(t)$ is usually measured macroscopically through the extravasation of MRI agents (Gd-DTPA) into the tissue. This function substantially depends on the molecular weight of administrated particle and needs to be scaled by $(1-0.5\log(M_{\mathrm{r}}))$ where M_{r} is the relative molecular weight of the administrated particles to the molecular weight of Gd-DTPA [8]. BBB closure time constant is also particle size-dependent and needs to be adapted to the therapeutic agent size as well [14].

To calculate the response of DNA-bound agents for a specific sonication spot, the model solves the system of ODEs given by (1)-(4) with the input function set as

$$I(t) = \frac{AD}{T_{\mathrm{inj}}} \operatorname{rect}(t, T_{\mathrm{inj}}), \tag{6}$$

where A is the inverse volume of distribution in plasma, D is the total injected dosage, and $\operatorname{rect}(t, T_{\mathrm{inj}})$ denotes the rectangular pulse-shaped function of duration T_{inj} starting at $t = 0$. It's important to note that while ultrasound exposure influences all reaction rate parameters, the model simplifies by assuming that only $K_{\mathrm{tv}}^{(n)}(t)$ is adjustable by ultrasound parameters. We need to sum up all the channel outputs to have a single output showing the amount of the drug delivered to the whole of the tumor. For simplicity, we assume the same transfer function for all the channels considering the same ultrasound exposure and vasculature density for all the sonication spots.

III. Channel characteristics

In this subsection, we examine our proposed ultrasound-enabled communication channel by defining classical communications inspired measures, i.e. *channel gain, transmission efficiency, signal-to-noise ratio (SNR)* and *bit error ratio (BER)*. The channel gain describes the transvascular rate enhancement due to the ultrasound exposure given by

$$\begin{aligned} G &= \int_0^\infty K_{\mathrm{tv}}(t)\,\mathrm{d}t - \int_0^\infty K_{\mathrm{tv}}^{\mathrm{b}}\,\mathrm{d}t \\ &= \left(K_{\mathrm{tv}}^{0} - K_{\mathrm{tv}}^{\mathrm{b}}\right)(t_0 + R). \end{aligned} \tag{7}$$

Also, the transmission efficiency of therapeutic agents through the channel is defined as

$$\eta^{(n)} = \frac{C_{\mathrm{b}}^{(n)}(\infty)d_{\mathrm{c}}}{\int_0^\infty I(t)\,\mathrm{d}t} = \frac{C_{\mathrm{b}}^{(n)}(\infty)d_{\mathrm{c}}}{AD}, \tag{8}$$

which shows the ratio of target cells DNA-bound drug to the total intravenously injected drug. The impact of drug systematic excretion as well as the efficiency of transvascular and transmembrane transport of the drug agents have been included in this parameter. In the context of the proposed

TABLE I: Model parameters and their units and values considered in this paper.

Symbol	Description	Value	Unit	Ref.
N	Number of channels	4		
T	Time between sequential sonication spots	15	min	
D	Total injected dosage	60×5.67	mg	[12]
A	Inverse volume of distribution in plasma	0.13×10^{-3}	1/mL	[12]
T_{inj}	Injection duration	30	min	
t_0	Sonication time	2	min	[5]
M	Molecular weight Gd-DTPA	938	g/mol	
$K_{\mathrm{tv}}^{\mathrm{b}}$	Baseline transvascular rate Gd-DTPA	0.003	min^{-1}	[6]
$K_{\mathrm{tv}}^{0,(n)}$	Sonicated transvascular rate Gd-DTPA(for 6 patients)	{0.0061 0.0045 0.0107 0.0173 0.0202 0.0113}	min^{-1}	[6]
R	Transvascular half-life Gd-DTPA	{2.45 2.14 3.33 4.59 5.14 3.44}	h	[15]
M	Molecular weight doxorubicin	543.5	g/mol	
$K_{\mathrm{tv}}^{\mathrm{b}}$	Baseline transvascular rate doxorubicin	0.0034	min^{-1}	
$K_{\mathrm{tv}}^{0,(n)}$	Sonicated transvascular rate doxorubicin (for 6 patients)	{0.0068 0.0050 0.0120 0.0194 0.0226 0.0126}	min^{-1}	
R	Transvascular half-life doxorubicin	{2.59 2.24 3.57 4.98 5.60 3.70}	h	
α	Volume fraction of ECM	0.4		[12]
$K_{\mathrm{d}}^{\mathrm{v}}$	Drug degradation in plasma	0.1462	min^{-1}	[15]
V	Rate of transmembrane transport	0.28	$\mathrm{ng}/(10^5\mathrm{cells})/\mathrm{min}$	[12]
d_{c}	Tumor cell density	$10^9(1-\alpha)$	cells/mL	[12]
K_{e}	The Michaelis constant for transmembrane transport	0.219	µg/mL	[12]
K_{i}	The Michaelis constant for transmembrane transport	1.37	$\mathrm{ng}/(10^5\mathrm{cells})$	[12]
$K_{\mathrm{d}}^{\mathrm{e}}$	Drug degradation rate in ECM	0.0301	min^{-1}	[15]
V_{b}	Binding rate of particles to DNA	0.0016	s^{-1}	[13]

SIMO system, we establish the SNR for the n^{th} channel by comparing the maximum drug delivery when the channel is subjected to ultrasound with the baseline scenario where there is no exposure to ultrasound:

$$\mathrm{SNR}^{(n)} = 10\log_{10}\frac{C_{\mathrm{b}}^{(n)}(\infty)}{C_{\mathrm{b}}^{\mathrm{b},(n)}(\infty)}. \tag{9}$$

The performance of modeled ultrasound-mediated chemotherapy and the eligibility of applied sonication parameters are assessed by SNR. We evaluate the outputs of each channel by comparing the final value of the delivered drug with a threshold. In the framework of a digital communication system, we detect bit 1 at the outputs when drug concentration exceeds the threshold and bit 0 if it is lower. We define the BER as the number of channels for which bit 0 is detected at output to the total number of channels given by

$$\mathrm{BER} = 1 - \frac{1}{N}\sum_{n=0}^{N-1}\left\{C_{\mathrm{b}}^{(n)}(\infty) \geq C_{\mathrm{target}}\right\}. \tag{10}$$

IV. Numerical Results

In this section, we elucidate the impact of ultrasound and injection parameters on channel characteristics. To accomplish this, we harness clinical data sourced from [6] related to the FUS treatment of six patients with Glioblastoma. Table I presents the model parameters including BBB transvascular coefficient for the six patients. We estimate the corresponding transvascular half-life R by linear fitting of the results reported in [15]. Our analysis focus on doxorubicin which is an anthracycline antibiotic that inhibits ribonucleic acid synthesis by binding to the tumor cells DNA, so transvascular rates and half-lifes are scaled accordingly.

Fig. 3 shows the time course of the vascular, extracellular, internalized and bound-to-DNA amount of doxorubicin for the four channel scenarios for patient 5. We sonicate the channels for two minutes one after another, at 0, 15, 30, and 45 min respectively, and start injecting the doxorubicin dosage at a constant rate at $t = 0$. During the 30 min injection time, the vascular concentration (Fig. 3a) increases. It is reduced only by degradation and by doxorubicin crossing the BBB. The influence of sonication is especially seen at $T = 15\,\mathrm{min}$ where the BBB opening leads to a drop in the vascular concentration. The extracellular concentration increases during the injection time (Fig. 3b). At the time of sonication, each channel shows a jump in concentration. This is especially lower for later sonicated channels due to a lower vascular concentration. Internalized doxorubicin over time shows a smoothed version of extracellular concentration due to the chemical reaction involved (Fig. 3c). The amount of bound doxorubicin to DNA increases at the beginning and converges approximately 100 min after injection (Fig. 3d). Thereby, later sonicated channels lead to a lower level. In the following we want to investigate the treatment by our proposed communication-inspired measures. Fig. 4 shows the results with respect to the six different patient scenarios. Since R increases with K_{tv}^{0}, a higher transvascular rate under sonication leads to a larger channel gain (4a). Consequently, patient 5 has the largest channel, i.e., the largest BBB opening. Please note that in this work the transvascular function is assumed to be the same for all four channels. Comparing the transmission efficiency (Fig. 4b) relatively between the respective channels reflects the final level observations in Fig. 3d. When sonication opens the BBB only slightly as in the case of patients 1 and 2, the efficiency of the channels is close to each other and close to the baseline scenario without sonication. Interestingly, increasing BBB opening leads to a worsening of the efficiency of the fourth channel, since a major part of doxorubicin has already been taken up by the

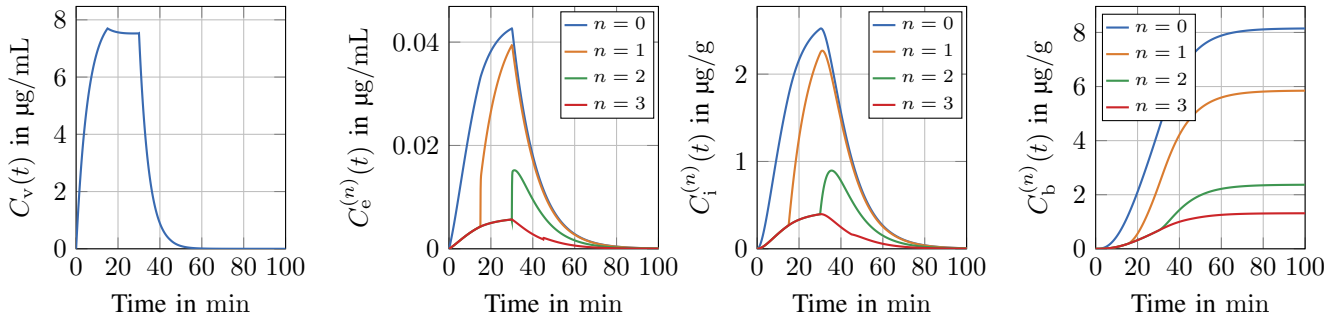

(a) (b) (c) (d)

Fig. 3: (a) vascular doxorubicin concentration, (b) extracellular doxorubicin concentration, (c) internalized doxorubicin, and (d) DNA-bound doxorubicin for patient 5 scenario in Table I.

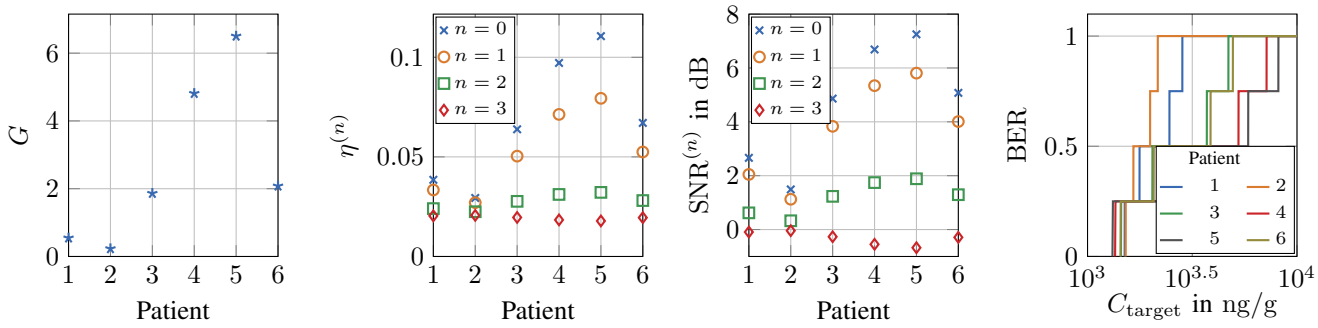

(a) (b) (c) (d)

Fig. 4: Patient dependent (a) channel gain, (b) transmission efficiency, (c) SNR, and (d) BER for the scenario in Table I.

other channels. This effect depends strongly on the injection duration and the time between sonications and can even be prevented, as it will be shown in the later analysis. The SNR results (Fig. 4c) underline these results. A large BBB opening leads to negative SNR for the fourth channel, i.e. to a deterioration compared to the scenario without sonication. Please note that we are either sonicating all channels or none. If only the fourth channel is not sonicated, the SNR would decrease further, as there is still a small gain achieved by sonication. The BER obtained depends strongly on the number of DNA-bound doxorubicin needed for a therapeutic effect (Fig. 4d). To obtain the lowest possible BER, it may be advantageous to open the BBB less by sonication so that all channels have sufficient doxorubicin available. In the scenario under investigation, the fourth channel is the bottleneck and a lower BBB opening leads to a higher C_{target} margin for an error-free system.

Fig. 5 and Fig. 6 show the effect of injection time and time between sonications on our communication-inspired measures. Note that channel gain is not presented since we hold t_0 constant. Increasing T_{inj} while keeping total injection dosage constant degrades the transmission efficiency and SNR of the first channel. But this degradation is small compared to the gain of the other channels and still the largest. Consequently, as T_{inj} increases, the BER curve shifts further to the right for the lower BER regimes. These observations claim that an injection of the drug over a longer period of time is advantageous. The opposite effect can be observed by varying T. A faster change between sonication spots leads to a degradation of the transmission efficiency and the SNR for the first channel, while the measures for the other channels improve. Consequently, the BER curve for low BER regimes shifts further to the right with a lower T. These results claim that switching as fast as possible between sonication spots is advantageous.

V. Conclusion

An ultrasound-enabled MC channel is introduced and characterized in this paper. The channel establishes a pathway from the intravenously injected drug to a hallmarked spot on the brain tumor utilizing the FUS to disrupt BBB. We proposed communication-inspired measures to quantify multi-target multi-sonication brain cancer therapy in the framework of a SIMO system. We demonstrate that ultrasound exposure can provide up to $8\,\mathrm{dB}$ SNR for the first channel but it degrades around $9\,\mathrm{dB}$ for the channel enabled with a $45\,\mathrm{min}$ time delay. The suggested channel model has been simplified to focus solely on the specific influence of ultrasound exposure on transvascular transport. However, there is room for enhancement by taking into account the broader impact of sonication output on additional mechanisms, such as cell-agent interactions and drug degradation rates within the ECM. This model could be exploited to maximize efficacy of Glioblastoma treatment considering clinically controlled parameters

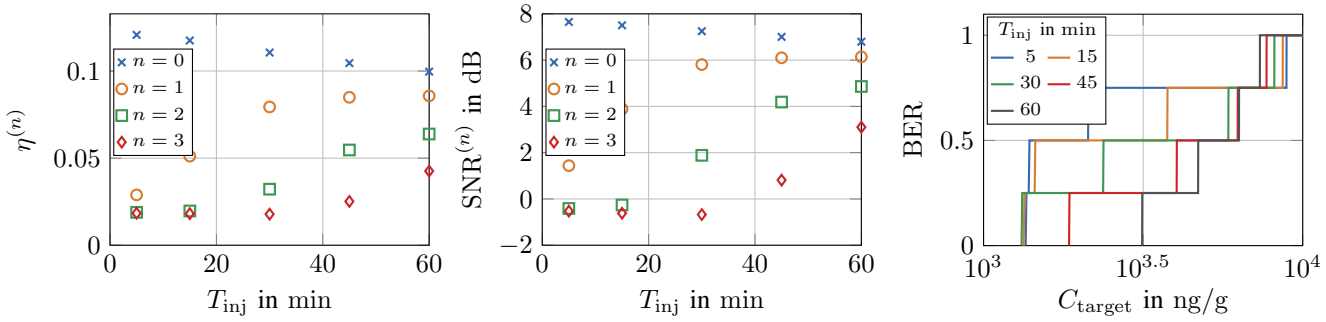

(a) (b) (c)

Fig. 5: Injection time dependent (a) transmission efficiency, (b) SNR, and (c) BER for the patient 5 scenario in Table I.

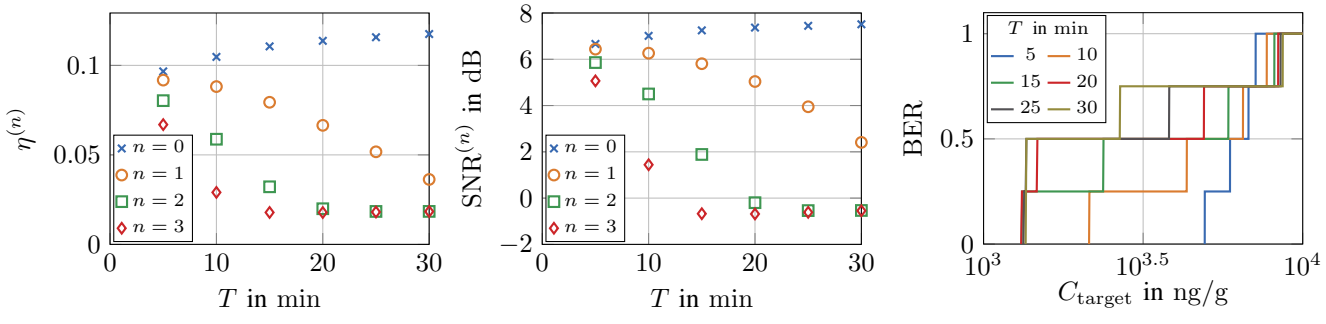

(a) (b) (c)

Fig. 6: (a) transmission efficiency, (b) SNR, and (c) BER w.r.t. time between sonications for the patient 5 scenario in Table I.

such as the drug injection time and delay between sonications. Adjusting these parameters could also be remarked in the future to reduce the augmented permeability in peripheral areas (healthy tissue) due to sonicating the tumor.

References

[1] Y. Zhao, P. Yue, Y. Peng, Y. Sun, X. Chen, Z. Zhao, and B. Han, "Recent advances in drug delivery systems for targeting brain tumors," *Drug Delivery*, vol. 30, no. 1, pp. 1–18, 2023.

[2] R. Rao, A. Patel, K. Hanchate, E. Robinson, A. Edwards, S. Shah, D. Higgins, K. J. Haworth, B. Lucke-Wold, D. Pomeranz Krummel *et al.*, "Advances in focused ultrasound for the treatment of brain tumors," *Tomography*, vol. 9, no. 3, pp. 1094–1109, 2023.

[3] S.-K. Wu, C.-L. Tsai, Y. Huang, and K. Hynynen, "Focused ultrasound and microbubbles-mediated drug delivery to brain tumor," *Pharmaceutics*, vol. 13, no. 1, p. 15, 2020.

[4] K. Gandhi, A. Barzegar-Fallah, A. Banstola, S. B. Rizwan, and J. N. Reynolds, "Ultrasound-mediated blood–brain barrier disruption for drug delivery: A systematic review of protocols, efficacy, and safety outcomes from preclinical and clinical studies," *Pharmaceutics*, vol. 14, no. 4, p. 833, 2022.

[5] J. Shin, C. Kong, J. S. Cho, J. Lee, C. S. Koh, M.-S. Yoon, Y. C. Na, W. S. Chang, and J. W. Chang, "Focused ultrasound–mediated noninvasive blood-brain barrier modulation: Preclinical examination of efficacy and safety in various sonication parameters," *Neurosurgical Focus*, vol. 44, no. 2, p. E15, 2018.

[6] K.-T. Chen, W.-Y. Chai, Y.-J. Lin, C.-J. Lin, P.-Y. Chen, H.-C. Tsai, C.-Y. Huang, J. S. Kuo, H.-L. Liu, and K.-C. Wei, "Neuronavigation-guided focused ultrasound for transcranial blood-brain barrier opening and immunostimulation in brain tumors," *Science Advances*, vol. 7, no. 6, p. eabd0772, 2021.

[7] N. A. Lapin, K. Gill, B. R. Shah, and R. Chopra, "Consistent opening of the blood brain barrier using focused ultrasound with constant intravenous infusion of microbubble agent," *Scientific reports*, vol. 10, no. 1, p. 16546, 2020.

[8] T. Nhan, A. Burgess, L. Lilge, and K. Hynynen, "Modeling localized delivery of doxorubicin to the brain following focused ultrasound enhanced blood-brain barrier permeability," *Physics in Medicine & Biology*, vol. 59, no. 20, p. 5987, 2014.

[9] U. A. Chude-Okonkwo, R. Malekian, B. T. Maharaj, and A. V. Vasilakos, "Molecular communication and nanonetwork for targeted drug delivery: A survey," *IEEE Communications Surveys & Tutorials*, vol. 19, no. 4, pp. 3046–3096, 2017.

[10] T. Nakano, S. Kobayashi, T. Suda, Y. Okaie, Y. Hiraoka, and T. Haraguchi, "Externally controllable molecular communication," *IEEE Journal on Selected Areas in Communications*, vol. 32, no. 12, pp. 2417–2431, 2014.

[11] H. Elayan, A. Eckford, and R. Adve, "Regulating molecular interactions using terahertz communication," in *ICC 2020-2020 IEEE International Conference on Communications (ICC)*. IEEE, 2020, pp. 1–6.

[12] A. W. El-Kareh and T. W. Secomb, "A mathematical model for comparison of bolus injection, continuous infusion, and liposomal delivery of doxorubicin to tumor cells," *Neoplasia*, vol. 2, no. 4, pp. 325–338, 2000.

[13] C. D. Arvanitis, V. Askoxylakis, Y. Guo, M. Datta, J. Kloepper, G. B. Ferraro, M. O. Bernabeu, D. Fukumura, N. McDannold, and R. K. Jain, "Mechanisms of enhanced drug delivery in brain metastases with focused ultrasound-induced blood–tumor barrier disruption," *Proceedings of the National Academy of Sciences*, vol. 115, no. 37, pp. E8717–E8726, 2018.

[14] B. Marty, B. Larrat, M. Van Landeghem, C. Robic, P. Robert, M. Port, D. Le Bihan, M. Pernot, M. Tanter, F. Lethimonnier *et al.*, "Dynamic study of blood–brain barrier closure after its disruption using ultrasound: a quantitative analysis," *Journal of Cerebral Blood Flow & Metabolism*, vol. 32, no. 10, pp. 1948–1958, 2012.

[15] J. Park, M. Aryal, N. Vykhodtseva, Y.-Z. Zhang, and N. McDannold, "Evaluation of permeability, doxorubicin delivery, and drug retention in a rat brain tumor model after ultrasound-induced blood-tumor barrier disruption," *Journal of Controlled Release*, vol. 250, pp. 77–85, 2017.